Measurement of nuclear excitation functions for proton induced reactions ($E_p = ???–55$ MeV) on natural Fe

Andrew S. Voyles,[1,*] Eric F. Matthews,[1] M. Shamsuzzoha Basunia,[2] Lee A. Bernstein,[2,1] Jonathan W. Engle,[3,†] Stephen A. Graves,[4] Amanda M. Lewis,[1] and Alexander Springer[5]

[1] *Department of Nuclear Engineering, University of California, Berkeley, Berkeley, CA 94720, USA*
[2] *Nuclear Science Division, Lawrence Berkeley National Laboratory, Berkeley, CA 94720, USA*
[3] *Department of Medical Physics, University of Wisconsin – Madison, Madison, WI 53705, USA*
[4] *Department of Radiation Oncology, University of Iowa, Iowa City, IA 52242, USA*
[5] *Fakultät für Physik, Karlsruhe Institute of Technology, 76131 Karlsruhe, Germany*

(Dated: May 9, 2018)

An article usually includes an abstract, a concise summary of the work covered at length in the main body of the article.

use the optional argument of the `\item` command to give the category of each item.

TODO LIST

I. INTRODUCTION

Blah blah blah

Novel applications are being explored for several radionuclides whose production methodologies are not established, but their production requires accurate, high-fidelity cross section data.

II. EXPERIMENTAL METHODS AND MATERIALS

The work described herein follows the methods utilized in our recent work and established by Graves *et al.* for monitor reaction characterization of beam energy and fluence in stacked target irradiations [1, 2]. Preliminary analysis was previously reported in the Master's thesis of one co-author, but the conclusive results of this work are described here [3].

ASV: Do we really need to cite Alex's thesis?

A. Stacked-target design

ASV: Update these energies, post-analysis

A pair of target stacks were constructed for this work, due to the large energy range desired to be spanned. One stack covers the 55–20 MeV range and the other covers 25–5 MeV, to minimize the systematic uncertainties associated with degradation of beam energy. In addition, the complementary energy of the stacks helps build confidence through multiple overlapping measurements between 20–25 MeV. A series of nominal 25 µm ^{nat}Fe foils (99.5%), 25 µm ^{nat}Ti foils (99.6%), and 25 µm ^{nat}Cu foils (99.95%) were used (all from Goodfellow Corporation, Coraopolis, PA 15108, USA) targets were used. In each stack, seven foils of each metal were cut down to 2.5×2.5 cm squares and characterized — for each foil, length and width measurements were taken at four different locations using a digital caliper (Mitutoyo America Corp.), thickness measurements were taken at four different locations using a digital micrometer (Mitutoyo America Corp.), and four mass measurements were taken using an analytical balance after cleaning the foils with

* andrew.voyles@berkeley.edu
† jwengle@wisc.edu

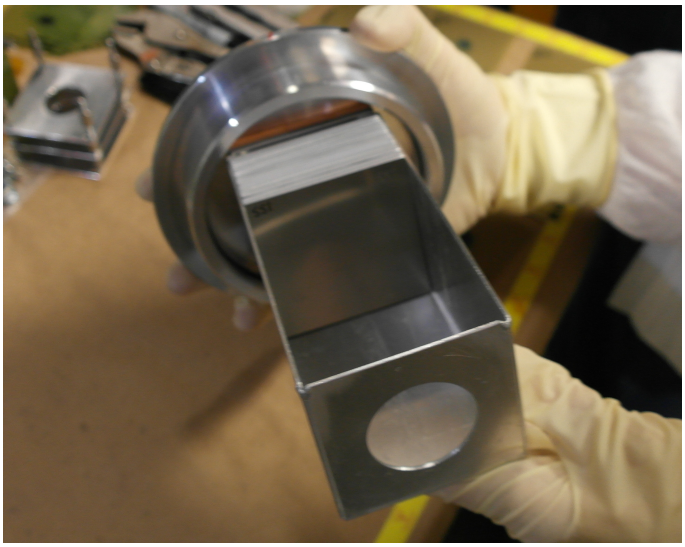

Figure 1. Photograph of the assembled 25 MeV target stack, before it was mounted in the beamline. The proton beam enters through the circular entrance in the foreground, and the upstream stainless steel profile monitor is visible at the front of the stack.

isopropyl alcohol. Using these length, width, and mass readings, the areal density and its uncertainty (in mg/cm^2) for each foil was calculated. The foils were tightly sealed into "packets" using two pieces of 3M 1205-Series Kapton polyimide film tape — each piece of tape consists of 38.1 µm of an acrylic adhesive (nominal 4.49 mg/cm^2) on 25.4 µm of a polyimide backing (nominal 3.61 mg/cm^2). The sealed foils were mounted over the hollow center of a 1.5875 mm-thick aluminum frame. Targets of 6061 aluminum alloy serve as proton energy degraders between energy positions. The target box, seen in Figure 1, is machined from 6061 aluminum alloy, and mounts on the end of an electrically-isolated beamline. The specifications of both target stack designs for this work are presented in Table I.

Both target stacks were assembled and separately irradiated at the Lawrence Berkeley National Laboratory (LBNL), using the 88-Inch Cyclotron, a K=140 sector-focused cyclotron. The 25 MeV stack was irradiated for approximately 20 minutes with a nominal current of 100 nA, for an anticipated integral current of 31.61 nAh. The 55 MeV stack was irradiated for approximately 10 minutes with a nominal current of 120 nA, for an anticipated integral current of 20.78 nAh. The beam current, measured using a current integrator on the electrically-isolated beamline, remained stable under these conditions for the duration of each irradiation. The proton beam incident upon each stack's upstream stainless steel profile monitor had a maximum energy of either 25 or 55 MeV, with an approximately 1.5% energy width due to multi-turn extraction — these energy profiles were used for all later analysis. Following end-of-bombardment (EoB), each stack was removed from the beamline and disassembled. All activated foils were transported to a counting lab for gamma spectrometry, which started approximately 30 minutes following the end of each irradiation.

B. Quantification of induced activities

A single detector was used in this measurement, an ORTEC GMX Series (model #GMX-50220-S) High-Purity Germanium (HPGe) detector. The detector is a nitrogen-cooled coaxial n-type HPGe with a 0.5 mm beryllium window, and a 64.9 mm diameter, 57.8 mm long crystal. Samples were counted at fixed positions ranging 5–60 cm (5% maximum permissible dead-time) from the front face of the detector, with a series of standard calibration sources used to determine energy and efficiency for each position. The foils were counted for a period of 4 weeks following end-of-bombardment (EoB), to accurately quantify all induced activities. For all spectra collected, net peak areas were fitted using the gamma spectrometry analysis code FitzPeaks [4], which utilizes the SAMPO fitting algorithms for gamma ray spectra [5].

The net counts in each fitted gamma-ray photopeak were converted into activities for the decaying activation products, using calibrated detector efficiencies and gamma-ray intensities for each transition. The nuclear decay data used in this work is tabulated, for reference, in Table II and Table III of Appendix A. Corrections for gamma-ray attenuation within each foil packet were made, using photon attenuation coefficients from the XCOM photon cross sections database [6]. The total propagated uncertainty in activity is the quadrature sum of the uncertainty in fitted peak areas, uncertainty in detector efficiency calibration, and uncertainty in the gamma-ray branching ratio data.

Table I. Specifications of the 25 MeV and 55 MeV target stack designs in the present work. The proton beam enters the stack upstream of the SS-5 and SS-3 profile monitors, respectively, and is transported through the stack in the order presented here. The 6061 aluminum degraders have a measured density of approximately 2.69 g/cm^3. Their areal densities were determined using the variance minimization techniques described in this work and the earlier paper by Graves *et al.* [2]. A 316 stainless steel foil is inserted at both the front and rear of each target stack as a monitor of the beam's spatial profile, by developing radiochromic film (Gafchromic EBT3) after end-of-bombardment (EoB).

25 MeV Target layer	Measured thickness	Measured areal density (mg/cm^2)	Uncertainty in areal density (%)	55 MeV Target layer	Measured thickness	Measured areal density (mg/cm^2)	Uncertainty in areal density (%)
SS profile monitor SS-5	130.94 µm	100.57	0.17	SS profile monitor SS-3	130.9 µm	100.48	0.17
Fe-08	26.25 µm	19.69	0.17	Fe-01	25.75 µm	20.22	0.21
Ti-14	25.01 µm	10.87	0.36	Ti-01	25.88 µm	11.09	0.16
Cu-14	24.01 µm	17.49	0.40	Cu-01	28.81 µm	22.40	0.11
Al Degrader E-09	256.5 µm	–	–	Al Degrader A-1	2.24 mm	–	–
Fe-09	26.5 µm	19.90	0.09	Fe-02	25.5 µm	19.91	0.13
Ti-15	23.81 µm	10.97	0.11	Ti-02	25.74 µm	10.94	0.24
Cu-15	21.81 µm	17.63	0.46	Cu-02	28.75 µm	22.32	0.40
Al Degrader H-01	127.09 µm	–	–	Al Degrader A-2	2.24 mm	–	–
Fe-10	26.5 µm	19.84	0.11	Fe-03	25.25 µm	20.00	0.27
Ti-16	24.6 µm	10.96	0.32	Ti-03	25.91 µm	11.25	0.15
Cu-16	22.01 µm	17.22	0.25	Cu-03	28.86 µm	22.49	0.20
Fe-11	27.26 µm	19.96	0.17	Al Degrader C-1	0.97 mm	–	–
Ti-17	25.01 µm	10.88	0.25	Fe-04	25.25 µm	19.93	0.33
Cu-17	29 µm	21.91	0.33	Ti-04	25.84 µm	10.91	0.18
Fe-12	27.01 µm	20.03	0.12	Cu-04	28.78 µm	22.38	0.29
Ti-18	25.01 µm	11.00	0.87	Al Degrader C-2	0.97 mm	–	–
Cu-18	28.75 µm	22.33	0.14	Fe-05	25.64 µm	20.02	0.24
Fe-013	26.25 µm	20.05	0.16	Ti-05	25.86 µm	10.99	0.30
Ti-19	26.6 µm	11.01	0.22	Cu-05	28.77 µm	22.35	0.12
Cu-19	28.75 µm	22.32	0.19	Al Degrader C-3	0.97 mm	–	–
Fe-14	25.75 µm	20.11	0.19	Fe-06	25.75 µm	20.21	0.26
Ti-20	27.01 µm	11.06	0.35	Ti-06	25.5 µm	11.15	0.23
Cu-20	28.26 µm	22.34	0.28	Cu-06	28.83 µm	22.43	0.10
SS profile monitor SS-6	131.5 µm	100.99	0.17	Al Degrader C-4	0.97 mm	–	–
				Fe-07	25.76 µm	19.93	0.19
				Ti-07	25.75 µm	11.17	0.33
				Cu-07	28.76 µm	22.34	0.24
				Al Degrader H-02	127.04 µm	–	–
				SS profile monitor SS-4	131.21 µm	101.25	0.16

As in our previous work, these activities used to calculate cross sections, and are differentiated between cumulative and independent [1]. For the first observable product nuclei in a mass chain, its (p,x) cross section will be reported as a cumulative cross section (σ_c), which is the sum of direct production of that nucleus, as well as decay of its precursors and any other independent cross sections leading to that nucleus. Cumulative cross sections will be reported whenever it is impossible to use decay spectrometry to distinguish independent production of a nucleus from decay feeding. For all remaining observed reaction products in the mass chain, and cases where no decay precursors exist, independent cross sections (σ_i) will be reported, allowing for determination of the independent production via subtraction and facilitating comparison to reaction model calculations. Solutions to the first- and higher-order Bateman equations are used for separation of feeding contributions from decay precursors, that independent cross sections may be reported [7, 8].

C. Proton fluence determination

Blah blah blah

D. Proton transport calculations

Blah blah blah

E. Calculation of measured cross sections

Blah blah blah

III. RESULTS AND DISCUSSION

Blah blah blah

IV. CONCLUSIONS

Blah blah blah

V. ACKNOWLEDGEMENTS

The authors would like to particularly acknowledge the assistance and support of (mention staff of the 88)

This work has been carried out under the auspices of the U.S. Department of Energy by Lawrence Berkeley National Laboratory and the U.S. Nuclear Data Program under contract # DE-AC02-05CH11231. This research was performed under appointment to the Rickover Fellowship Program in Nuclear Engineering, sponsored by the Naval Reactors Division of the U.S. Department of Energy Additional support has been provided by the U.S. Nuclear Regulatory Commission.

This research used the Savio computational cluster resource provided by the Berkeley Research Computing program at the University of California, Berkeley (supported by the UC Berkeley Chancellor, Vice Chancellor for Research, and Chief Information Officer).

Appendix A: Decay data

The lifetimes and gamma-ray branching ratios listed in these tables were used for all calculations of measured cross sections reported in this work, and have been taken from the most recent edition of Nuclear Data Sheets for each mass chain

Table II. Decay data for gamma-rays observed in ^{nat}Ti(p,x) and ^{nat}Cu(p,x).

Nuclide	Half-life	E_γ (keV)	I_γ (%)
^{22}Na	2.6018(22) y	1274.537	99.940(14)

Table III. Decay data for gamma-rays observed in ^{nat}Fe(p,x).

Nuclide	Half-life	E_γ (keV)	I_γ (%)
^{82m}Rb	6.472(6) h	554.35	62.4(9)
	6.472(6) h	619.11	37.98(9)

Appendix B: Measured excitation functions

Figures of the cross sections measured in this work are presented here, in comparison with literature data

Appendix C: Measured isomer-to-ground state branching ratios

Plots of the isomer-to-ground state ratios measured in this work are presented here, in comparison with literature data and reaction modeling codes

---

[1] A. S. Voyles, L. A. Bernstein, E. R. Birnbaum, J. W. Engle, S. A. Graves, T. Kawano, A. M. Lewis, and F. M. Nortier, (2018), arXiv:1804.06548.

[2] S. A. Graves, P. A. Ellison, T. E. Barnhart, H. F. Valdovinos, E. R. Birnbaum, F. M. Nortier, R. J. Nickles, and J. W. Engle, Nuclear Instruments and Methods in Physics Research, Section B: Beam Interactions with Materials and Atoms **386**, 44 (2016).

[3] A. Springer, (2017), arXiv:1707.05908.

[4] J. Fitzgerald, "FitzPeaks gamma analysis and calibration software," (2009).

[5] P. A. Aarnio, M. T. Nikkinen, and J. T. Routti, Journal of Radioanalytical and Nuclear Chemistry **248**, 371 (2001).

[6] M. J. Berger, J. H. Hubbell, S. M. Seltzer, J. Chang, J. S. Coursey, R. Sukumar, D. S. Zucker, and K. Olsen, (2010).

[7] H. Bateman, in *Proc. Cambridge Philos. Soc*, Vol. 15 (1910) pp. 423–427.

[8] J. Cetnar, Annals of Nuclear Energy **33**, 640 (2006).